Available online at www.sciencedirect.com
SCIENCE DIRECT®
ELSEVIER
Physica D 185 (2003) 45–66
PHYSICA D
www.elsevier.com/locate/physd

Boolean dynamics of networks with scale-free topology

Maximino Aldana*

James Franck Institute, The University of Chicago, 5640 South Ellis Avenue, Chicago, IL60637, USA

Received 16 January 2003; accepted 23 May 2003
Communicated by R.E. Goldstein

Abstract

The dynamics of Boolean networks with scale-free topology are studied. The existence of a phase transition from ordered to chaotic dynamics, governed by the value of the scale-free exponent of the network, is shown analytically by analyzing the overlap between two distinct trajectories. The phase diagram shows that the phase transition occurs for values of the scale-free exponent in the open interval (2, 2.5). Since the Boolean networks under study are directed graphs, the scale-free topology of the input connections and that of the output connections are studied separately. Ultimately these two topologies are shown to be equivalent. A numerical study of the attractor structure of the configuration space reveals that this structure is similar in both networks with scale-free topologies and networks with homogeneous random topologies. However, an important result of this work is that the fine-tuning usually required to achieve stability in the dynamics of networks with homogeneous random topologies is no longer necessary when the network topology is scale-free. Finally, based on the results presented in this work, it is hypothesized that the scale-free topology favors the evolution and adaptation of network functioning from a biological perspective.

PACS: 05.45.+b; 87.10.+e; 64.60.Cn; 64.60.Ht

Keywords: Boolean networks; Scale-free topology; Dynamical phase transition; Stability; Evolvability

1. Introduction

The study and characterization of the statistical properties of complex networks has received renewed attention in the last few years [1,27]. In particular, it has been recently shown by Barabási, Newman, Solé and many other authors that a great variety of real networks exhibit a scale-free topology, including the WWW and the Internet [2], social networks [21], metabolic and protein networks [14,15,23], ecological networks [8,24], and genetic networks [12,22], to mention just a few examples (for more references see [1,6]). A scale-free topology means that the probability $P(k)$ that an arbitrary element of the network is connected to exactly k other elements has the form $P(k) = Ck^{-\gamma}$, where γ is usually called the *scale-free exponent*. Scale-free networks have the key property that a small fraction of the elements are highly connected, whereas the majority of the elements are poorly connected. The ubiquity of scale-free networks in nature has led to a systematic study of the structural properties that characterize the wiring diagram of these networks. Nevertheless, the dynamics generated by a scale-free network topology when the elements are provided with some kind of dynamic interaction rule, remain essentially unexplored.

* Tel.: +1-773-7020946; fax: +1-773-7022172.
E-mail address: maximino@control.uchicago.edu (M. Aldana).

0167-2789/$ – see front matter © 2003 Elsevier B.V. All rights reserved.
doi:10.1016/S0167-2789(03)00174-X

An interesting dynamical network in which the scale-free topology has important implications is the N–K model proposed by Stuart Kauffman in 1969 to describe generically the dynamics involved in the processes of gene regulation and cell differentiation [16]. In this classic model, the genome of a given organism is represented by a set of N genes, each being a binary variable describing the two possible states of gene-expression: either the gene is expressed (1) or it is not (0). Since the expression of a gene is controlled by the expression of some other genes, Kauffman assumed the genome as a directed network in which a link from a given gene A to another gene B means that A controls the expression of B. In view of the complexity exhibited by real genetic networks, Kauffman made three simplifying assumptions: (a) every gene is controlled by (is connected to) exactly K other genes; (b) the K genes to which every gene is connected are chosen randomly with uniform probability from the entire system; (c) each gene is expressed with probability p and is not expressed with probability $1 - p$, depending upon the configurations of its K controlling genes.

Even with these simplifying assumptions, a very rich and unexpected behavior of the model was found (for references see [5]). In particular, in 1986 Derrida and Pomeau showed analytically the existence of a dynamical phase transition controlled by the parameters K and p [10]. For every value of p, there exists a critical value of the connectivity, $K_c(p) = [2p(1-p)]^{-1}$, such that if $K < K_c(p)$ all perturbations in an initial state of the system die out (ordered phase). For $K > K_c(p)$ a small perturbation in the initial state of the system propagates across the entire system over time (chaotic phase). According to Kauffman, Stauffer, and other authors, only when $K = K_c(p)$ (the critical phase) does the N–K model have the required stability properties compatible with the order manifest in the genetic networks of living organisms [17,26]. This fact made Kauffman coin the term “life at the edge of chaos” to refer to networks functioning at the critical phase.

Although the N–K model qualitatively points in the right direction, it fails to account for a quantitative description of what actually is observed in genetic networks. One of the main problems is that the critical connectivity $K_c(p)$ is very small for most values of p (see Fig. 1). In contrast, it is well known that real genetic networks exhibit a wide range of connectivities. For example, the expression of the human β-globine gene (expressed in red blood cells) or the *even-skipped* gene in *Drosophila* (playing an impor-

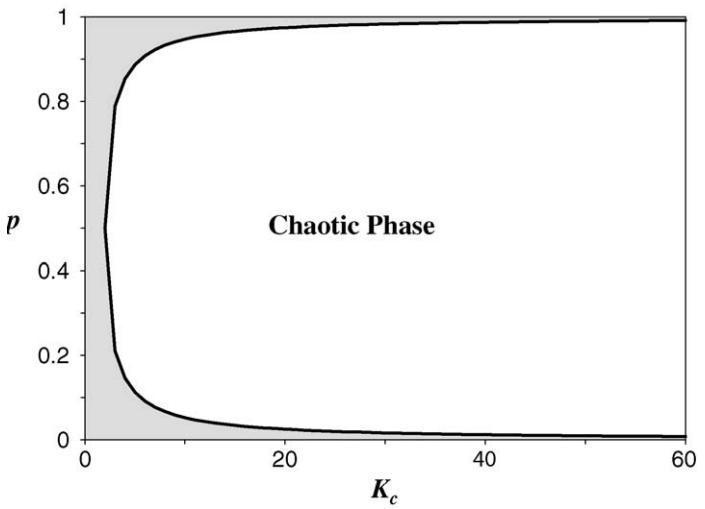

Fig. 1. Phase diagram for the standard N–K model. The solid curve is the critical connectivity K_c as a function of p given by Eq. (8). The shaded area represents the ordered phase ($K < K_c$), whereas the white area represents the chaotic phase ($K > K_c$).

tant role in the development of the embryo), are each controlled by more than 20 different regulatory proteins [4]. Analogously, both the fibroblast growth factor (FGF) activation and the platelet-derived growth factor (PDGF) activation in mammalian cells, result in the cascade activation of over 60 other genes [13]. On the other side of the spectrum is the *lac* operon in *E. coli*, which is regulated by only two proteins: the *lac* repressor protein and the catabolite activator protein [4]. These observations are contrary to the Kauffman model since high connectivities imply either chaotic behavior or almost constant Boolean functions (p very close to 0 or 1). To achieve stability with moderately high connectivities in the N–K model, it is necessary to fine-tune the value of p. For instance, in order to have stable dynamics when the critical connectivity is $K_c = 20$, the value of p should be in the interval $0 < p < 0.026$ (or $0.974 < p < 1$). As far as we can tell, there is neither a theoretical nor an experimental reason justifying why the parameters K and p should "live" in, or at the edge of, the shaded area of Fig. 1.

The above suggests that the random network topology upon which the Kauffman model is based, is inadequate. In view of the ubiquity of scale-free networks and of the fact that some genes in real genetic networks are highly connected whereas others are not, it is reasonable to replace assumptions (a) and (b) mentioned above by the assumption that the connectivity k of every gene in the network follows a scale-free distribution, $P(k) \sim k^{-\gamma}$. It was not until very recently that the dynamics of the N–K model with a scale-free topology were studied numerically [12,22]. Nevertheless, the values of γ and p at which the phase transition occurs, if it does occur at all, were unknown in these previous works and the results may have to be reinterpreted. The main purpose of this work is to show that the N–K model with scale-free topology does indeed exhibit a dynamical phase transition from ordered to chaotic behaviors, and to determine how this topology affects the stability of the dynamics.

This paper is organized as follows. In the next section, we present the N–K model and explain how different network topologies can be implemented on it. In Section 3, we show analytically that the N–K model with scale-free topology undergoes a phase transition controlled by the scale-free exponent γ and the parameter p, and provide the phase diagram that fully identifies the ordered, critical, and chaotic phases. Since the N–K model is a directed graph, in Section 4 we analyze two cases: (a) the topology of the input connections of the network is scale-free, whereas the topology of the output connections is homogeneously random, and (b) vice-versa. It is analytically shown in Section 5 that these two cases are dynamically equivalent in the sense that they produce the same phase diagram. The attractor structure of the configuration space is analyzed in Section 5. We present numerical results about the relevant quantities that characterize the attractors and their basins of attraction (such as the attractor length and the number of different basins of attraction) for each one of the three dynamical phases, ordered, critical, and chaotic. Our results indicate that the structure of the configuration space is qualitatively similar in both scale-free networks and networks with homogeneous random architectures. In Section 6, we analyze the robustness of the dynamics by forcing an arbitrary element of the network to disregard its controlling elements and to produce a random output. We show that the stability of the dynamics under this kind of random perturbation depends on the connectivity of the node that is perturbed: the higher the connectivity of the perturbed element, the more unstable the system is. We conclude in Section 7 with a discussion of the results and their possible implications for biological systems.

2. The N–K model

The model which we will be working with is the following. The network is represented by a set of N Boolean variables (or elements), $\{\sigma_1, \sigma_2, \ldots, \sigma_N\}$, that can take on the values 0 or 1. Each element σ_i is controlled by k_i other elements of the network, where k_i is chosen randomly from a probability distribution $P_{\text{in}}(k)$. We will call k_i the *connectivity* of the ith element of the network. The k_i elements $\{\sigma_{i_1}, \ldots, \sigma_{i_{k_i}}\}$

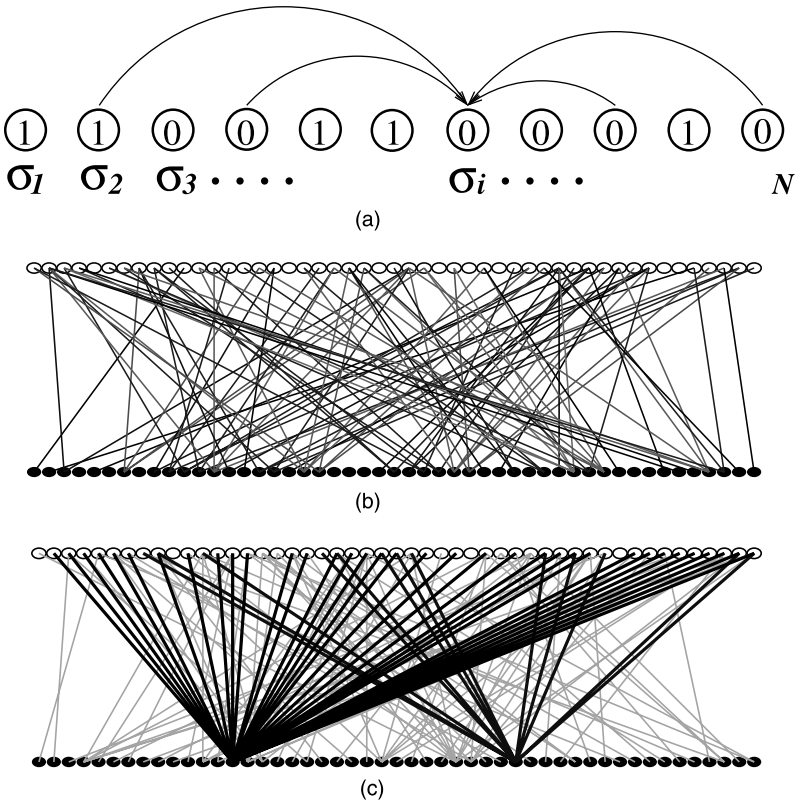

Fig. 2. Schematic representation of the N–K model architecture. (a) Every element σ_i receives inputs from k_i other elements. $k_i = 4$ for the particular element σ_i depicted on the figure. (b) A typical realization of the network architecture for a Poissonian distribution of the input connections with mean value $K = 2$. In this diagram the black circles are the elements of the network, whereas the white circles represent the input elements. (c) Same kind of diagram as before but in this case the distribution of input connections is scale-free with $\gamma = 2.5$ (and a corresponding mean value $K_\gamma \approx 2$).

that control the state of σ_i are chosen randomly with uniform probability from anywhere in the system (see Fig. 2a). There are different possibilities for $P_{\text{in}}(k)$, each giving rise to different network topologies. Two important cases are:

- The *homogeneous random topology*, in which every element of the network is statistically equivalent to any other one. A representative example of this kind of topology is given by the probability distribution $P_{\text{in}}(k) = \mathrm{e}^{-K}K^k/k!$, $K > 0$. Although in this case the number of connections per element changes from one element to another, the network topology can be meaningfully characterized by the average connectivity K since the probability of having elements with connectivities much different from K is negligible.[1] The above is illustrated in Fig. 2b, which shows a typical realization of the network topology generated by a Poissonian distribution with mean value $K = 2$. In this article, we will refer to the N–K model with homogeneous random topology as the *standard N–K model*.
- The *scale-free topology*, for which $P_{\text{in}}(k) = [\zeta(\gamma)k^\gamma]^{-1}$, where $\gamma > 1$ and $\zeta(\gamma) = \sum_{k=1}^{\infty} k^{-\gamma}$ is the Riemann Zeta function. This probability distribution gives rise to a network topology

[1] Another equivalent topology is given by the probability distribution $P_{\text{in}}(k) = \delta(k - K)$, where $\delta(k)$ is the Dirac delta function and K is a positive integer. This probability distribution corresponds to the original model proposed by Kauffman [16].

characterized by a wide heterogeneity in the connectivity of the elements. Although for $\gamma > 2$ the mean value of the connectivity is finite and given by $K_\gamma = \zeta(\gamma-1)/\zeta(\gamma)$, it is useless to characterize the network topology. The above is illustrated in Fig. 2c, which shows a typical realization of the network topology for $\gamma = 2.5$ and a corresponding mean connectivity $K_\gamma \approx 1.95$. As can be seen from this figure, the connectivity of the elements ranges from one to almost the size of the system. Therefore, a mean connectivity $K_\gamma \approx 1.95$ tells nothing about the network architecture. The only relevant parameter to characterize this topology is the scale-free exponent γ. We will refer to the N–K model with scale-free topology as the *scale-free N–K model*.

Once a set $\{\sigma_{i_1}, \ldots, \sigma_{i_{k_i}}\}$ of k_i controlling elements has been assigned to every element σ_i of the network, we need to specify how these elements will determine the value of σ_i at every time-step. In order to do so, we assign to each σ_i a Boolean function, $f_i(\sigma_{i_1}, \ldots, \sigma_{i_{k_i}})$, such that for each configuration of the controlling elements, $f_i = 1$ with probability p and $f_i = 0$ with probability $1-p$. The specification of the controlling elements and Boolean functions for all the elements σ_i, $i = 1, 2, \ldots, N$, is called a *network realization*. Once a network realization has been established, the values of the elements are synchronously updated according to the dynamical equation:

$$\sigma_i(t+1) = f_i(\sigma_{i_1}(t), \ldots, \sigma_{i_{k_i}}(t)). \tag{1}$$

We will denote as Σ_t the configuration of the entire system at time t, namely, $\Sigma_t = \{\sigma_1(t), \sigma_2(t), \ldots, \sigma_N(t)\}$. With this notation the dynamical equation can be written as

$$\Sigma_{t+1} = \mathcal{F}[\Sigma_t], \tag{2}$$

where $\mathcal{F}$ is a shorthand that represents the action of the set of Boolean functions $\{f_1, f_2, \ldots, f_N\}$ on the configuration Σ_t. We will say that, under the above dynamics, Σ_t is the *precursor* of Σ_{t+1}.

3. The phase diagram of the scale-free N–K model

3.1. Computation of the phase diagram

To show the existence of the phase transition, we consider the overlap $x(t)$ between two distinct configurations, $\Sigma_t = \{\sigma_1(t), \sigma_2(t), \ldots, \sigma_N(t)\}$ and $\tilde{\Sigma}_t = \{\tilde{\sigma}_1(t), \tilde{\sigma}_2(t), \ldots, \tilde{\sigma}_N(t)\}$. (The temporal evolution of these two configurations is governed by the same set of Boolean functions.) The overlap is defined as the fraction of elements in both configurations that have the same value, and is given by

$$x(t) = 1 - \frac{1}{N}\sum_{i=1}^{N} |\sigma_i(t) - \tilde{\sigma}_i(t)|. \tag{3}$$

If Σ_t and $\tilde{\Sigma}_t$ are totally independent, then $x(t) \approx 0.5$, whereas if they are almost equal $x(t) \approx 1$. In the limit $N \to \infty$, the overlap becomes the probability for two arbitrary but corresponding elements, $\sigma_i(t) \in \Sigma_t$ and $\tilde{\sigma}_i(t) \in \tilde{\Sigma}_t$, to be equal. The stationary value of the overlap, defined as $x = \lim_{t\to\infty} x(t)$, can be considered as an order parameter of the system. If $x = 1$, the system is insensitive to initial perturbations (all differences between configurations die out over time). In this case the system presents an ordered behavior. On the other hand, if $x \neq 1$, the initial perturbations propagate across the entire system and do not disappear. The system then exhibits chaotic behavior.

To find a dynamical equation for the overlap, we generalize the annealed computation carried out by Derrida and Pomeau in [10] to the case in which each element σ_i receives k_i inputs with probability $P_{\text{in}}(k_i)$. For completeness we reproduce here this calculation.

Let $\mathcal{A}_t$ be the set of the elements that at time t are equal in both configurations, Σ_t and $\tilde{\Sigma}_t$. Analogously, let $\mathcal{B}_t$ be the set of all those elements that are different. The overlap $x(t)$ is just the number of elements contained in $\mathcal{A}_t$ divided by N. There are two possibilities for the k_i input elements of an arbitrary element $\sigma_i(t)$:

- All the k_i inputs of $\sigma_i(t)$ belong to $\mathcal{A}_t$. In this case, which occurs with probability $[x(t)]^{k_i}$, the probability that $\sigma_i(t+1) = \tilde{\sigma}_i(t+1)$ is exactly one since the Boolean function f_i has the same input values for both $\sigma_i(t)$ and $\tilde{\sigma}_i(t)$.

- At least one of the k_i inputs of $\sigma_i(t)$ belongs to $\mathcal{B}_t$, which occurs with probability $1-[x(t)]^{k_i}$. In this case, $\sigma_i(t+1) = \tilde{\sigma}_i(t+1)$ only if the output of the Boolean function f_i is the same for both elements even when they have different input values. From the definition of the Boolean functions it follows that the probability of having $f_i(\sigma_{i_1}(t),\ldots,\sigma_{i_{k_i}}(t)) = f_i(\tilde{\sigma}_{i_1}(t),\ldots,\tilde{\sigma}_{i_{k_i}}(t))$, regardless of the values of the inputs in each configuration, is $p^2+(1-p)^2$.

Therefore, the probability $x(t+1)$ that $\sigma_i(t+1) = \tilde{\sigma}_i(t+1)$ is given by

$$x(t+1) = \sum_{k_i=1}^{\infty} \{[x(t)]^{k_i} + (1-[x(t)]^{k_i}) \times (p^2+(1-p)^2)\} P_{\text{in}}(k_i). \tag{4}$$

Rearranging terms and using the fact that $\sum_{k=1}^{\infty} P_{\text{in}}(k) = 1$, we find that the overlap obeys the dynamical equation:

$$x(t+1) = M(x(t)), \tag{5}$$

where the mapping $M(x)$ is given by

$$M(x) \equiv 1 - 2p(1-p)\left\{1 - \sum_{k=1}^{\infty} x^k P_{\text{in}}(k)\right\}. \tag{6}$$

In the limit $t \to \infty$, Eq. (5) becomes the fixed point equation $x = M(x)$ for the stationary value of the overlap. Note that $x = 1$ is always a fixed point of Eq. (5). Nonetheless, this solution may be stable or unstable depending on $P_{\text{in}}(k)$. Note also that $M(x)$ is a monotonically increasing function of x with the property that $M(0) = 1-2p(1-p)$ and $M(1) = 1$. Therefore, Eq. (5) will have a stable fixed point $x^* \neq 1$ only if $\lim_{x\to 1^-} \mathrm{d}M(x)/\mathrm{d}x > 1$ (chaotic phase). In contrast, if $\lim_{x\to 1^-} \mathrm{d}M(x)/\mathrm{d}x < 1$ the only fixed point is $x = 1$ (ordered phase). The situation is illustrated in Fig. 3. The phase transition between the ordered and chaotic regimes occurs when $\lim_{x\to 1^-} \mathrm{d}M(x)/\mathrm{d}x = 1$. From Eq. (6) it follows that

$$\lim_{x\to 1^-} \frac{\mathrm{d}M(x)}{\mathrm{d}x} = 2p(1-p)\sum_{k=1}^{\infty} kP_{\text{in}}(k) = 2p(1-p)K, \tag{7}$$

where $K = \sum_{k=1}^{\infty} kP_{\text{in}}(k)$ is the first moment of $P_{\text{in}}(k)$. The phase transition is then determined by the condition:

$$2p(1-p)K = 1. \tag{8}$$

It is interesting to note that the phase transition is governed only by the first moment of $P_{\text{in}}(t)$. Nevertheless,

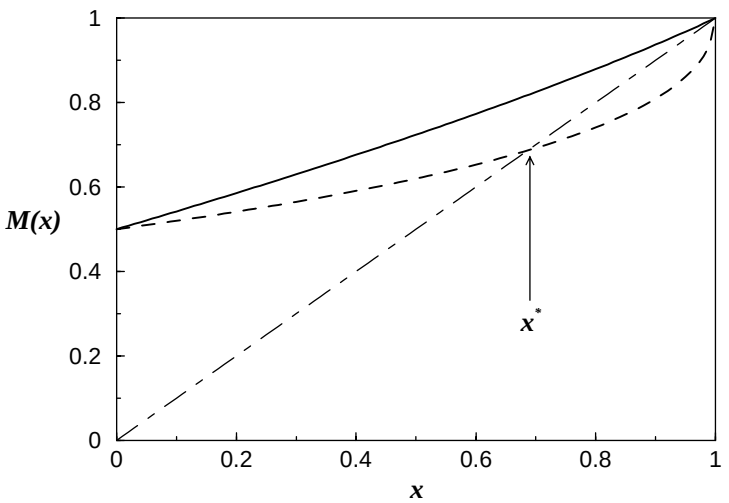

Fig. 3. Plot of the mapping $M(x)$ as a function of x for a scale-free distribution $P_{\text{in}}(k) \sim k^{-\gamma}$. The solid curve corresponds to $\gamma = 3$, for which $\lim_{x\to 1^-} \mathrm{d}M(x)/\mathrm{d}x < 1$. The only fixed point in this case is $x = 1$. The dashed curve corresponds to $\gamma = 1.5$, for which $\lim_{x\to 1^-} \mathrm{d}M(x)/\mathrm{d}x = \infty$. In this last case there is a fixed point $x^* \neq 1$. The dashed-dotted line is the identity.

for the scale-free distribution $P_{\text{in}}(k) = [\zeta(\gamma)k^{\gamma}]^{-1}$, the first moment is not necessarily a meaningful parameter to characterize the network topology. For instance, if $2 < \gamma \leq 3$, the second moment of the distribution is infinite even when the first moment has a finite value, which means that the fluctuations around the first moment are much larger than the first moment itself. Therefore, rather than characterizing the phase transition using the first moment of the distribution, we will do it by means of the scale-free exponent γ, which is the only natural parameter that determines the network topology.

For the scale-free distribution to be normalizable, it is necessary to have $\gamma > 1$. Under such conditions, the first moment K_{γ} of this distribution is then expressed as a function of γ as

$$K_{\gamma} = \begin{cases} \infty & \text{if } 1 < \gamma \leq 2, \\ \dfrac{\zeta(\gamma - 1)}{\zeta(\gamma)} & \text{if } \gamma > 2. \end{cases} \tag{9}$$

From Eqs. (7)–(9), it follows that the fixed point $x = 1$ is unstable if $1 < \gamma \leq 2$. In this case, Eq. (5) has a stable fixed point $x^* \neq 1$, and the system is in the chaotic phase for any value of p in the open interval (0, 1). The only way in which the overlap between two distinct configurations can converge to 1 is if all the Boolean functions are constant, namely, if either $p = 0$ or $p = 1$. On the other hand, when $\gamma > 2$ the first moment of the distribution is finite. In this case, the value γ_c of the scaling-free exponent at which the phase transition occurs is determined by the transcendental equation:

$$2p(1-p)\frac{\zeta(\gamma_c - 1)}{\zeta(\gamma_c)} = 1. \tag{10}$$

The values γ_c and p for which this equation is satisfied are plotted in Fig. 4. As can be seen, $\gamma_c \in [2, 2.5]$ for any value of p. Actually, γ_c reaches its maximum value $\gamma_c^{\max} \approx 2.47875$ at $p = 0.5$. Above this maximum value the system is always in the ordered phase regardless of the value or p.

3.2. Scale-free exponents of real networks

Interestingly, it happens that $\gamma \in [2, 2.5]$ for the majority of real scale-free networks that have been analyzed. For example, Fig. 5 shows the histogram of 30 different scale-free exponents reported in [1,20,25] for a wide collection of scale-free networks (not too many more networks have been analyzed so far). This collection includes not only biological networks, but also social, ecological and informatics networks. Although these networks follow dynamics that may be different

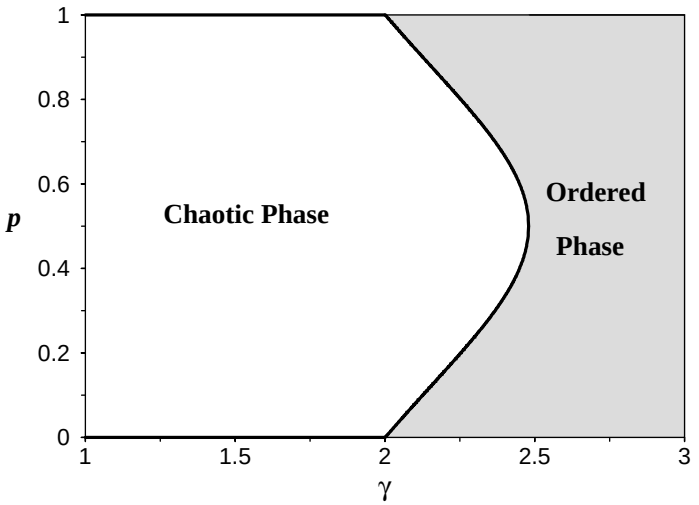

Fig. 4. Phase diagram for the scale-free N–K model. The solid line is the value of γ_c as a function of p given by the transcendental equation (10). The white and shaded areas represent the chaotic phase ($\gamma < \gamma_c$) and the ordered phase ($\gamma > \gamma_c$), respectively.

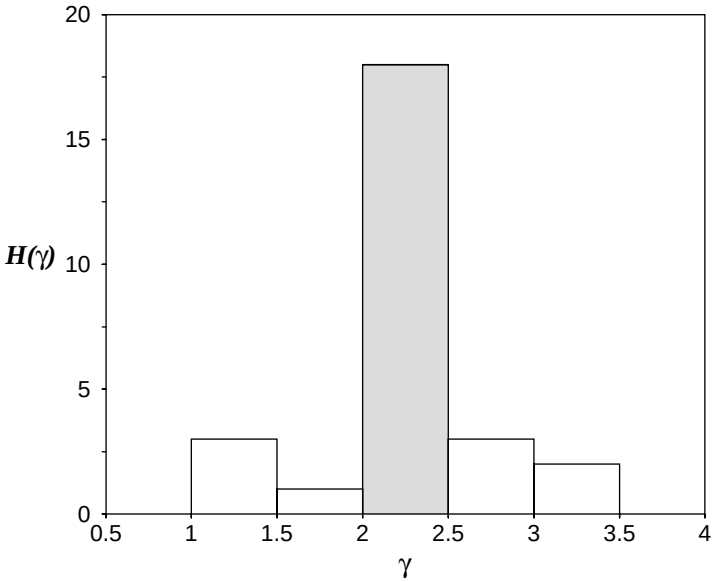

Fig. 5. Histogram of values of the critical exponent γ for a collection of 30 scale-free networks reported in the literature (see [1,20,25]). Note that the majority of the exponents in this collection of networks fall in the interval [2, 2.5], in which the phase transition predicted by Eq. (10) occurs.

from the Boolean dynamics considered in this article, it is remarkable that the majority of these exponents (66%) fall in the interval on which the phase transition of the scale-free N–K model occurs.

3.3. Comparison with the standard N–K model

In the standard N–K model all the elements have more or less the same connectivity, $k_i \approx K\,\forall i$, and Eq. (8) reduces to the result obtained by Derrida and Pomeau in [10].[2] The values of K and p for which Eq. (8) is satisfied are plotted in Fig. 1. Note that the phase diagram of the standard N–K model is totally dominated by the chaotic phase. This does not occur for the scale-free N–K model, as shown in Fig. 4. In the scale-free N–K model, the ordered phase extends from $\gamma = 2$ up to $\gamma = \infty$, whereas the chaotic phase is confined to the interval $1 < \gamma < 2.47875$.

It is worth noting that the limit $\gamma \to \infty$ in the scale-free N–K model corresponds to the case $K = 1$ for the standard N–K model. Indeed, the nth moment $K_\gamma^{(n)}$ of the scale-free distribution $P_\gamma(k) = [\zeta(\gamma)k_\gamma]^{-1}$ is given by

$$K_\gamma^{(n)} = \sum_{k=1}^{\infty} k^n P_\gamma(k) = \frac{\zeta(\gamma - n)}{\zeta(\gamma)},$$

which in the limit $\gamma \to \infty$ becomes

$$\lim_{\gamma\to\infty} K_\gamma^{(n)} = 1 \quad \forall n.$$

The above result shows that in the limit $\gamma \to \infty$, the scale-free distribution $P_\gamma(k) = [\zeta(\gamma)k^\gamma]^{-1}$ transforms into the Dirac delta function $\delta(k-1)$, since in this limit these two distributions have exactly the same moments:

$$\lim_{\gamma\to\infty} P_\gamma(k) = \delta(k-1).$$

The standard N–K model with $K = 1$ was analytically solved by Flyvbjerg and Kjaer in [11], and the structure of the configuration space for this case is thoroughly known.

The opposite limit $K \to \infty$ of the standard N–K model was also solved analytically. It is equivalent to

[2] Luque and Solé derived Eq. (8) in [19] by considering the set of relevant elements of the system—the elements that do not reach a constant value over time.

the so-called *Random Map model* and gives rise to the maximum chaotic behavior of the system [9]. To establish the equivalence of the Random Map model and the scale-free N–K model it is not enough to require the divergence of the first moment K_γ of the scale-free distribution $P_\gamma(k) = [\zeta(\gamma)k^\gamma]^{-1}$. The reason is that K_γ diverges for any value of γ in the interval $1 < \gamma \leq 2$. However, the equivalence between the Random Map model and the scale-free N–K model can be obtained by analyzing the behavior of K_γ for *finite* systems.

For a finite system with N elements, the Random Map model is equivalent to the standard N–K model with $K = N$ [5,9]. In this case, when the size of the system goes to infinity, the mean connectivity K diverges linearly with N. To obtain the equivalence between the Random Map model and the scale-free N–K model we will impose the same condition, namely, the first moment K_γ of the scale-free distribution $P_\gamma(k)$ diverges linearly with N in the limit $N \to \infty$.

In the case of a finite system of size N, the scale-free distribution $P_\gamma(k)$ is given by

$$P_\gamma(k) = \frac{1}{\zeta(\gamma, N)} k^{-\gamma}, \quad k = 1, 2, \ldots, N,$$

where $\zeta(\gamma, N)$ is the incomplete Riemann Zeta function defined as

$$\zeta(\gamma, N) = \sum_{k=1}^{N} k^{-\gamma}.$$

The first moment K_γ is then given by

$$K_\gamma = \frac{\zeta(\gamma - 1, N)}{\zeta(\gamma, N)}.$$

From the above, it can be shown that K_γ has the following behavior for large values of N:

$$K_\gamma \sim \begin{cases} \ln N & \text{for } \gamma = 2, \\ \dfrac{N}{\ln N} & \text{for } \gamma = 1, \\ N & \text{for } \gamma = 0. \end{cases} \tag{11}$$

Therefore, even when K_γ diverges with N for any $\gamma \leq 2$, the divergence is linear only for $\gamma = 0$. For finite systems the Random Map model is recovered from the scale-free N–K model when $\gamma = 0$. However, for infinite systems the scale-free distribution $P_\gamma(k)$ fails to be normalizable if $\gamma \leq 1$ and the whole analysis presented in Section 3.2 is no longer meaningful. The minimum value of γ that gives chaotic behavior in infinite systems is $\gamma = 1$.

4. The N–K model is a directed graph

An important characteristic of the N–K model is that it is a directed graph: if σ_i is a controlling element of σ_j, the opposite does not necessarily occur. Every element σ_i is regulated by k_i elements. But σ_i can in turn regulate the value of a number of other elements, say l_i. The distribution $P_{\text{in}}(k)$ of input connections is not necessarily equal to the distribution $P_{\text{out}}(l)$ of output connections. Up to now we have assumed that $P_{\text{in}}(k)$ is scale-free, whereas $P_{\text{out}}(l)$ is Poissonian, as in Fig. 2c.[3] But it is also possible for the network of output connections to present a scale-free topology. To apply our previous results to the case in which $P_{\text{out}}(l)$ is known instead of $P_{\text{in}}(k)$, we should find how these two distributions are related.

Suppose now that an arbitrary element σ_i of the network has l_i outputs with probability $P_{\text{out}}(l_i) = l_i^{-\gamma}/\zeta(\gamma)$. (We assume that $\gamma > 2$ so that the first moment of the distribution is well defined.) It is easy to see that when the l_i outputs of every element are chosen randomly with uniform probability from anywhere in the system, the input probability distribution $P_{\text{in}}(k)$ is given by

$$P_{\text{in}}(k) = \binom{N}{k} \left(\frac{\langle l \rangle_{\text{out}}}{N}\right)^k \left(1 - \frac{\langle l \rangle_{\text{out}}}{N}\right)^{N-k}, \tag{12}$$

where $\langle l \rangle_{\text{out}}$ is the first moment of $P_{\text{out}}(l)$. In the limit $N \to \infty$, the above expression transforms into the distribution:

$$P_{\text{in}}(k) = \mathrm{e}^{-\langle l \rangle_{\text{out}}} \frac{[\langle l \rangle_{\text{out}}]^k}{k!}. \tag{13}$$

The above is a Poisson distribution whose first moment $\langle k \rangle_{\text{in}}$ is equal to the first moment of $P_{\text{out}}(l)$: $\langle k \rangle_{\text{in}} =$

[3] $P_{\text{out}}(l)$ turns out to be Poissonian since the k_i inputs of each σ_i are chosen randomly with equal probability from anywhere in the system.

$\langle l \rangle_{\text{out}}$. This result is expected since the total number of input connections in the network is exactly the same as the total number of output connections. Therefore, the mean of the inputs equals the mean of the outputs. Since only the first moment of the input distribution appears in Eq. (8), the above result shows that the phase diagram depicted in Fig. 4 is still valid if either $P_{\text{in}}(k)$ or $P_{\text{out}}(l)$ are scale-free. In view of this result, in what follows we will consider only the case in which $P_{\text{in}}(k)$ is scale-free and $P_{\text{out}}(l)$ is Poissonian. There is still a third possibility: that *both* $P_{\text{in}}(k)$ and $P_{\text{out}}(l)$ are scale-free. We will not consider this situation here.

5. Structure of the configuration space

For a finite value of N, there is a total of $\Omega = 2^N$ possible dynamical configurations of the network.[4] Since the configuration space is finite, starting from any initial state, the system will eventually return to a previously visited configuration, falling into a cyclic behavior thereafter. The set of configurations that constitute a cycle is usually called an *attractor* and the number of configurations it contains is the *attractor length*. All the configurations that eventually converge to an attractor constitute its *basin of attraction*. It is possible to have many attractors for a given realization of connections and Boolean functions. Although the dynamics given by Eq. (1) are deterministic, the relevant quantities that characterize the attractors and their basins of attraction are statistical in nature since they change from one network realization to another. Despite 30 years of research on the Kauffman model, an analytical determination of quantities such as the mean number of attractors, or the mean attractor length, is still eluding us. [5] However, a great deal of numerical work has been done to understand the structure of the configuration space of the Kauffman model (for references see [5]). Here, we present equivalent results for networks with scale-free topologies.

[4] For "dynamical configuration", we mean a particular realization of 0's and 1's of the set of variables $\{\sigma_1, \sigma_2, \ldots, \sigma_N\}$.

[5] It was possible to solve analytically the structure of the configuration space of the standard Kauffman model only for the cases $K = 1$ and $K = \infty$ (see [9,11]).

The numerical data presented in this section were computed by sampling all the $\Omega = 2^N$ configurations of the configuration space for a given network realization, and then averaging the quantity under consideration using 20,000 network realizations. Since the number of configurations grows exponentially with N, the biggest networks that we analyzed had $N = 19$ and $N = 20$ ($\Omega = 524{,}288$ and $\Omega = 1{,}048{,}576$ configurations, respectively). Each quantity that we analyzed was computed in this way for the three dynamical phases, using the values $p = 0.5$ and $\gamma = 1.1$ for the chaotic phase, $\gamma = \gamma_c = 2.47875$ for the critical phase, and $\gamma = 3$ for the ordered phase. Every time that we refer to the chaotic, critical and ordered phases without further specification of p and γ, we will mean these values of the parameters.

5.1. Basins of attraction

Fig. 6 shows typical structures of the configuration space for three networks with different values of the scale-free exponent, corresponding to the three phases shown in Fig. 4: the ordered phase, the critical phase, and the chaotic phase. The networks used to generate Fig. 6 consisted of $N = 10$ elements, which gives $\Omega = 2^{10} = 1024$ configurations. Similar pictures are displayed in Fig. 7 for a system with $N = 15$ ($\Omega = 32{,}768$). One can see from Figs. 6 and 7 that the structures of the attractors and their basins of attractions change considerably from one phase to another. For example, it is apparent from these figures that in the ordered and critical phases the vast majority of points have no precursors, whereas in the chaotic phase there are considerably more points having precursors. An immediate consequence of this fact is that the average *transient time*, namely, the mean time that it takes to reach the attractor starting out from an arbitrary configuration, is larger in the chaotic phase than in the ordered and critical phases.

The above statements can be made more quantitative by computing the probabilities $P_{\text{p}}(n_{\text{p}})$ and $P_\tau(\tau)$ that an arbitrary configuration has n_{p} precursors and a transient time τ, respectively. These probabilities are depicted in Figs. 8 and 9, for networks with $N = 19$ and different values of γ. In Fig. 8, we have suppressed

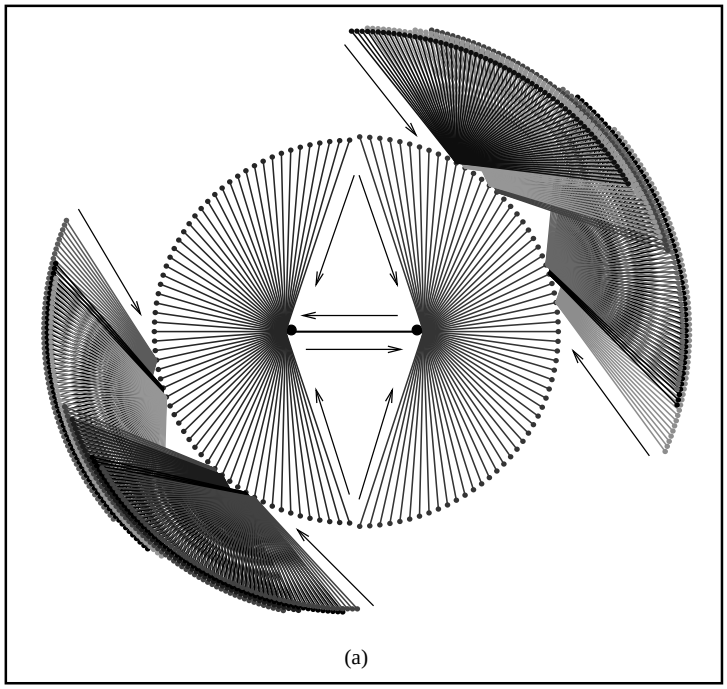

(a)

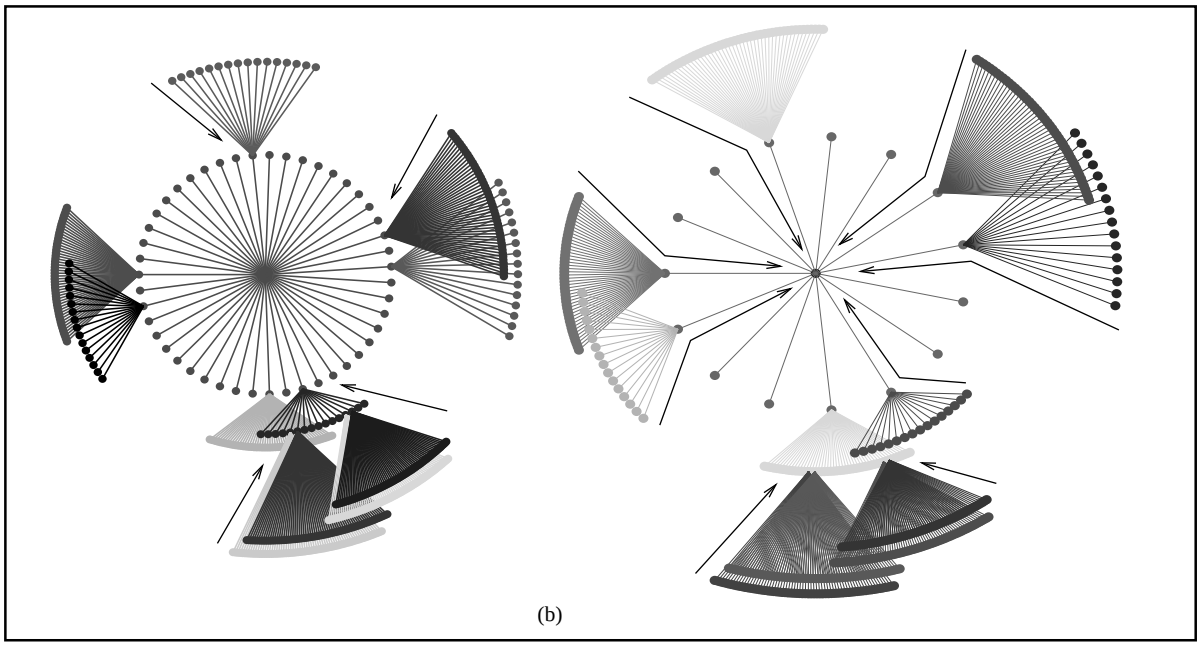

(b)

Fig. 6. Geometric representation of the structure of the configuration space of Boolean networks with scale-free topology. Each bold point corresponds to a dynamical configuration of the system. A link between any two points means that one point is the precursor of the other one. The arrows indicate the direction of the dynamical flow. The cases shown correspond to three different values of the scale-free exponent for networks with $N = 10$ elements ($\Omega = 1024$ configurations). (a) Ordered phase: there is only one attractor consisting of two points. Note that the vast majority of points (99.22%) do not have precursors. (b) Critical phase: there are two attractors, each consisting of only one point. (c) Chaotic phase: there are five attractors of different lengths. In this case approximately 10% of the points have precursors.

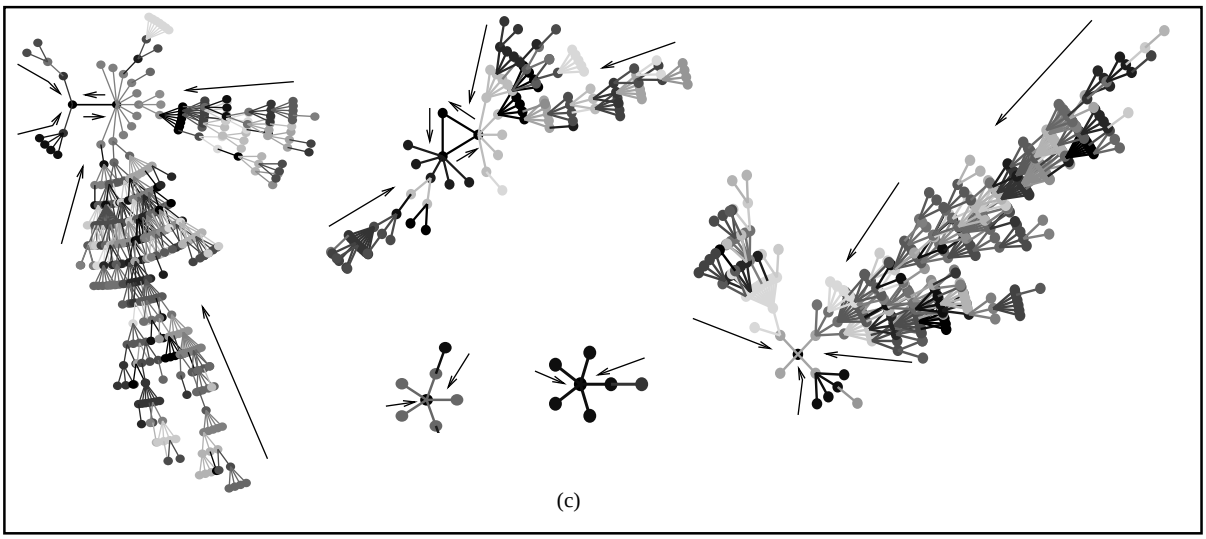

Fig. 6. (*Continued*).

the point $P_p(0)$ since it is much bigger than the rest of the points. $P_p(0)$ gives the probability that a randomly chosen configuration has no precursors, and its value is $P_p(0) \approx 0.90$ in the chaotic phase and $P_p(0) \approx 0.99$ in the critical and ordered phases. Focusing our attention only on the configurations that do have precursors, we can see that in the chaotic phase the majority of these configurations have between 1 and 10 precursors, whereas in the ordered and critical phases the number of precursors can be anything between 10 and 1000. Consequently, transient times can be much longer in the chaotic phase than in the ordered and critical phases, as Fig. 9 shows.

Another interesting quantity is the size of the basins of attraction, namely, the number of points that converge to the same attractor. Figs. 6 and 7 suggest that in the ordered and critical phases the basins of attraction are roughly of the same size, whereas in the chaotic phase they can contain from just a few points to almost the entire configuration space. The above can be seen in Fig. 10, which shows the probability $P_s(n_s)$ of having a basin of attraction of size n_s for networks with $N = 19$ and different values of γ. In the ordered and critical phases the probability $P_s(n_s)$ is mostly concentrated on the values $n_s = \Omega/2^r$, $r = 0, 1, \ldots, \infty$, and decreases rapidly as $r \to \infty$. Therefore, in random network realizations we would typically obtain attraction basins of sizes $n_s = \Omega$ and $n_s = \Omega/2$. Contrary to this, as we go deeper into the chaotic phase, $P_s(n_s)$ is less concentrated on the values $n_s = \Omega/2^r$. It spreads out over the whole interval $n_s \in [1, \Omega]$ (note the difference in scales on the Y-axis of the three graphs depicted in Fig. 10). For example, for $\gamma = 1.1$ the two largest values of $P_s(n_s)$ occur at $n_s = 1$ and $n_s = \Omega$, which is indicative of the enormous fluctuations of basin sizes that take place in the chaotic phase.

The above results account for the structures observed in Figs. 6 and 7. In the ordered and critical phases the basins of attraction are compact (short transients) and roughly of the same size, whereas in the chaotic phase there are basins of attraction with very long branches (long transients) that contain almost the entire configuration space, as well as very small ones with just a few points.

5.2. Attractors

There are two important quantities that characterize the attractors of the configuration space: the number n_a of different attractors in a particular network realization, and the attractor length l_a. These two quantities also change randomly from one network realization to

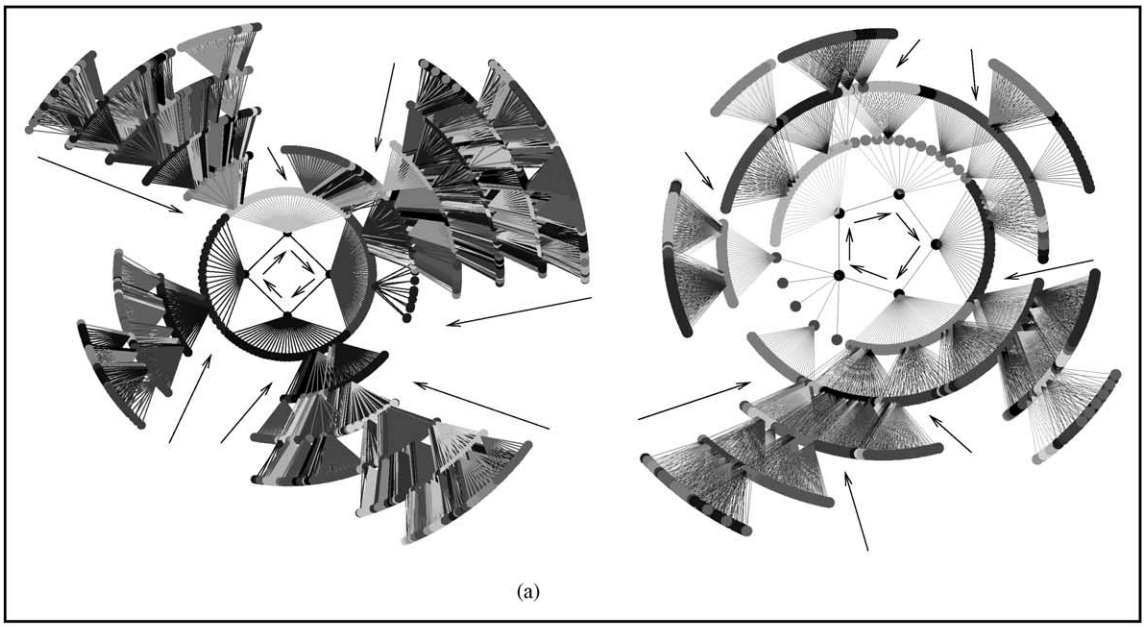

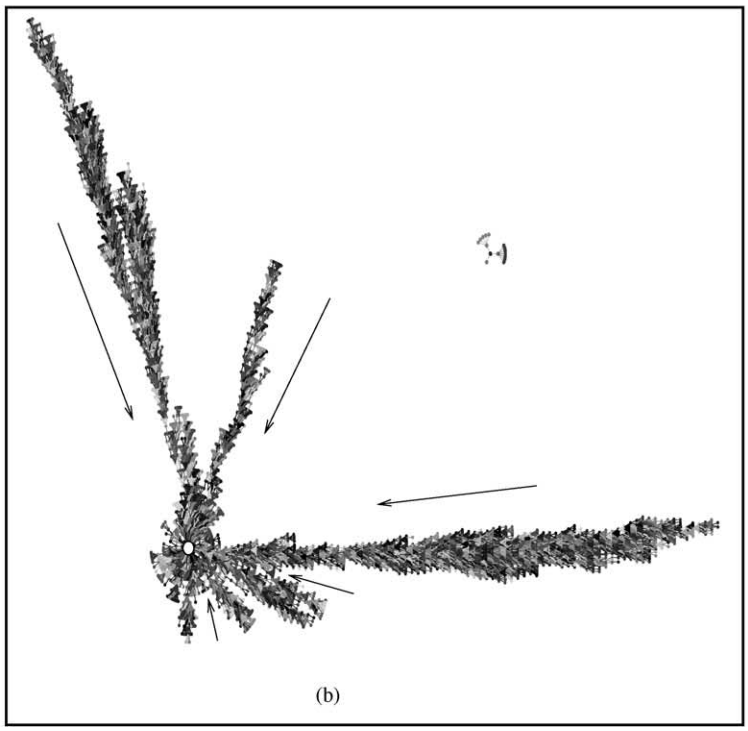

Fig. 7. Structure of the configuration space for networks with $N = 15$ ($\Omega = 32{,}768$). (a) Critical phase: there are two attractors of lengths 4 and 5. Note that the two basins of attraction are roughly of the same size. (b) Chaotic phase: there are also two attractors of lengths 16 (discernible as a small circle) and 1, but in this case the sizes of their basins of attraction are completely out of proportion. The attractors in (b) were drawn using a linear scale seven times smaller than the one used in (a).

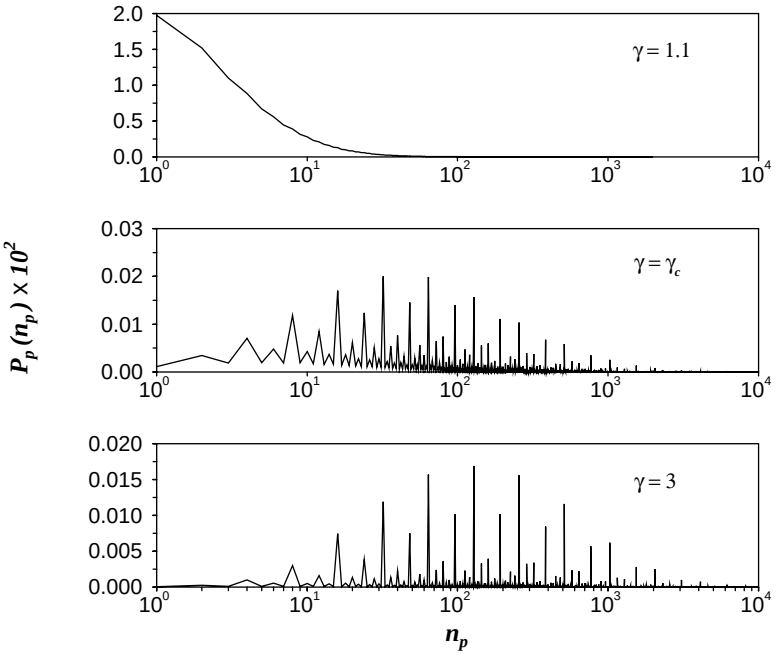

Fig. 8. Probability $P_{\mathrm{p}}(n_{\mathrm{p}})$ that an arbitrary configuration has n_{p} precursors in networks with $N = 19$ and different values of γ. The point $P_{\mathrm{p}}(0)$, corresponding to configurations with no precursors, has been excluded from the graphs since it is disproportionately larger than the rest of the points. ($P_{\mathrm{p}}(0) = 0.8974$ for $\gamma = 1.1$, $P_{\mathrm{p}}(0) = 0.9951$ for $\gamma = \gamma_{\mathrm{c}}$, and $P_{\mathrm{p}}(0) = 0.9974$ for $\gamma = 3$.) The prominent spikes in the two bottom graphs occur at values of n_{p} that are powers of 2.

another. Fig. 11 shows the probability $P_{\mathrm{a}}(n_{\mathrm{a}})$ of having n_{a} different attractors in an arbitrary network realization, whereas the probability $P_l(l_{\mathrm{a}})$ that a given attractor has a length l_{a} is plotted in Fig. 12. The data displayed on these figures were computed for networks with $N = 19$. As can be seen, the number of different attractors in a given network realization is typically bigger in the chaotic phase than in the critical and ordered phases. The same is true for the length of the attractors: in the chaotic phase $P_l(l_{\mathrm{a}})$ has a long tail that is not present in the critical and ordered phases.

The above results are of course related to the phase diagram shown in Fig. 4, which was computed by analyzing the stationary value of the overlap between two different configurations. We recall that in the ordered and critical phases two different initial configurations eventually converge to the same state (the overlap is $x = 1$), whereas in the chaotic phase these two configurations remain always different ($x \neq 1$). In the context of the structure of the configuration space, we see from Fig. 11 that in the ordered and critical phases we typically have only one attractor. Therefore, two initial configurations will typically converge to the same state just because they fall into the same attractor. On the other hand, in the chaotic phase we typically have more than one attractor. Consequently, two different initial configurations do not necessarily converge to the same state since they can fall into different attractors. Although the phase diagram depicted in Fig. 4 was computed by means of the annealed approximation for infinite systems, it reflects what actually happens in quenched-finite systems. As a matter of fact, the approximation gets better as the system size increases.

5.3. Mean quantities

So far we have analyzed the probability distributions of the main quantities that characterize the structure of the configuration space: the number of different attractors in a given network realization, the length of an arbitrary attractor and the transient time that it takes to

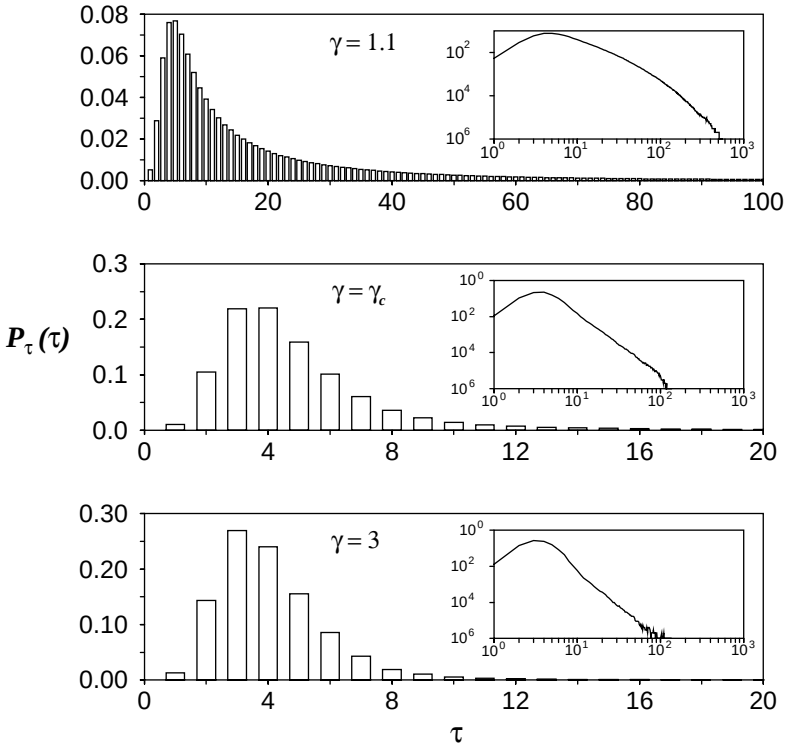

Fig. 9. Probability $P_\tau(\tau)$ of having a transient time τ when starting from an arbitrary configuration, for networks with $N = 19$. The insets are the same data as in the corresponding graph, but plotted in log–log coordinates.

reach the attractor starting out from an arbitrary configuration. In this subsection, we consider the *mean* values of these quantities. In particular, we are interested in how the mean values of the quantities mentioned above change with the size of the network.

Fig. 13a shows the mean value $\langle n_a \rangle$ of the number of different attractors as a function of the size of the system N for three values of the scale-free exponent, corresponding to the three dynamical phases. Note that in the three phases $\langle n_a \rangle$ grows linearly with N, although in average there are more attractors in the chaotic phase than in the ordered and critical phases, as should be expected.

On the other hand, Fig. 13b shows the mean attractor length $\langle l_a \rangle$ as a function of N, again for the same three values of γ. The important thing to note here is that $\langle l_a \rangle$ grows exponentially with N in the chaotic phase, whereas in the ordered and critical phases $\langle l_a \rangle$ grows linearly with N. The same is true for the mean transient time $\langle \tau \rangle$, as can be seen from Fig. 13c: $\langle \tau \rangle \sim e^{\alpha N}$ in the chaotic phase whereas $\langle \tau \rangle \sim N$ in the ordered and critical phases.

5.4. Comparison with the standard N–K model

The numerical results presented throughout this section for networks with scale-free topology reveal a structure of the configuration space that is completely analogous to the one obtained in the standard Kauffman model with homogeneous random topology. Almost every statement that we have made to describe any of the figures of this section would be qualitatively true if we were considering the standard N–K model.[6] This is good news because all the work done in the

[6] Although for many years it was believed that $\langle n_a \rangle \sim N^{1/2}$ in the critical phase of the standard Kauffman model, recent studies seem to confirm that $\langle n_a \rangle \sim N$ in the three phases [7], as in Fig. 13a.

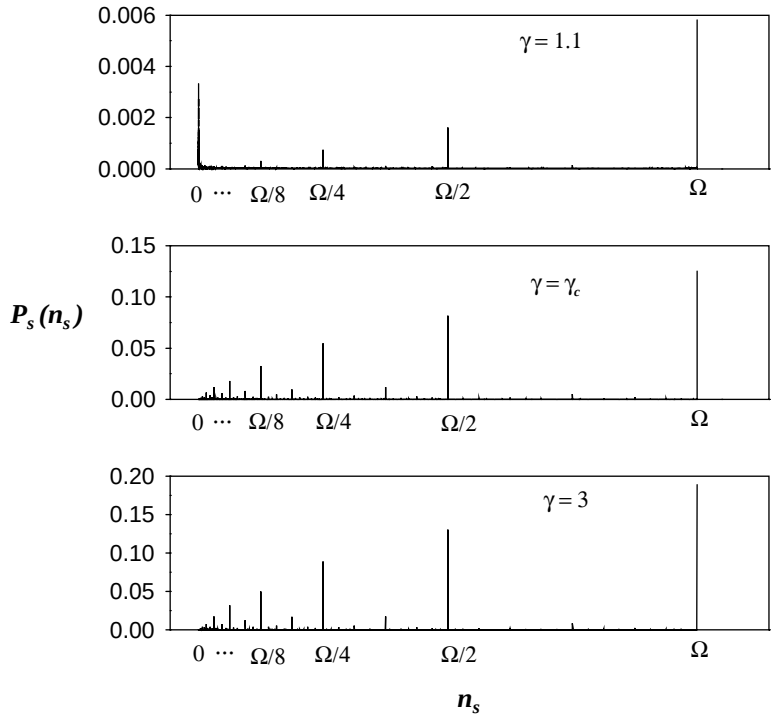

Fig. 10. Probability $P_s(n_s)$ of having a basin of attraction of size n_s, for networks with $N = 19$. In the ordered and critical phases $P_s(n_s)$ is mostly concentrated on the values $n_s = \Omega/2^r$, $r = 0, 1, 2, \ldots$. However, in the chaotic phase $P_s(n_s)$ spreads over all the intermediate values of n_s, which is reflected in the difference of scales on the Y-axis. For $\gamma = 1.1$ the two largest values of $P_s(n_s)$ occur at $n_s = \Omega$ and $n_s = 1$, whereas in the ordered and critical phases the two largest values occur at $n_s = \Omega$ and $n_s = \Omega/2$.

last three decades to understand the Boolean dynamics of networks with homogeneous random architectures could be applicable, at least qualitatively, to the case of scale-free networks. However, for the standard N–K model to operate in the ordered phase it is necessary that *all* the elements of the network have very small connectivities, or that the Boolean functions are almost constant. This restriction is not required when the network has a scale-free topology, for it can operate in the ordered phase even when some of its elements are highly connected. In addition, the wide heterogeneity in the connectivities of the elements of a scale-free network has an important consequence: the stability of the dynamics exhibited in the ordered and critical phases of the standard N–K model is of a quite different nature than the one exhibited in the corresponding phases of networks with scale-free topology. To put it in a metaphoric way, the "gray" of the shaded area (ordered phase) depicted in Fig. 1 is of a different hue than the "gray" of the ordered phase in Fig. 4. This is the topic of the next section.

6. Stability and evolvability

According to the biological interpretation of the Kauffman model, each attractor of the configuration space represents a particular biological task [18]. More specifically, each attractor represents a cell type or a cell fate. In this frame, cell reproduction processes start with an initial configuration of genes, $\Sigma_0 = \{\sigma_1(0), \sigma_2(0), \ldots, \sigma_N(0)\}$, determined by the cell's environment (chemical gradients). This configuration eventually falls into its corresponding attractor, which determines a particular cell type or cell fate. For the cell to perform its biological task with reliability, it is important that small perturbations in the initial configurations Σ_0 do not propagate

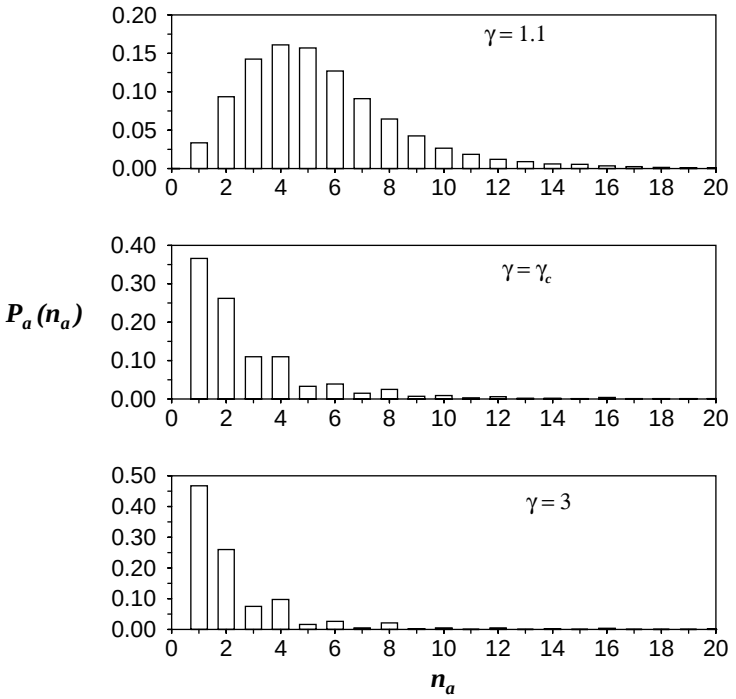

Fig. 11. Probability $P_a(n_a)$ of having n_a different attractors in a random network realization. The data were computed for networks with $N = 19$. Note that in the ordered and critical phases the most probable number of different attractors is $n_a = 1$, whereas in the chaotic phase it is $n_a = 4$.

over time to the entire system. Otherwise the system can "jump" from one attractor to a different one, changing the cell's fate. On the other hand, very deep into the ordered phase nothing changes since all perturbation in the initial configuration Σ_0, no matter how small or how large, die out over time preventing the cell from evolving. These considerations led Kauffman to hypothesize that the "optimal" networks for the modeling of living organisms lie along the critical phase, in which the system is not extremely sensitive to perturbations but it is not frozen either.

The above hypothesis, which is known as *life at the edge of chaos*, is based upon the assumption that all the elements of the network are statistically equivalent. So, perturbing an element is equivalent to perturbing any other one. Under such circumstances, the only way to change the stability of the system is by changing the mean connectivity K of the entire network, or by changing the value of the parameter p which is also associated to the entire network. But the above is no longer true for networks with scale-free topology. We do not expect that perturbing an element with a low connectivity has the same effect on the network dynamics than perturbing an element with a high connectivity, even in the ordered phase. It is true that in the ordered phase, especially for large values of γ, highly connected elements are rare. But they do exist. And it has been shown in [3] that the properties of a scale-free network change considerably when the highly connected elements are deliberately attacked. Therefore, it is important to consider the stability of the dynamics of the network when elements with different connectivities are perturbed. In order to do so, we force a given element of the network, say σ_i which has a connectivity k_i, to acquire the values 0 and 1 randomly at every time step with probability 1/2, regardless of the values of its controlling elements. In other words, we perturb *only one* element of the network, σ_i, by introducing a noisy signal that forces this

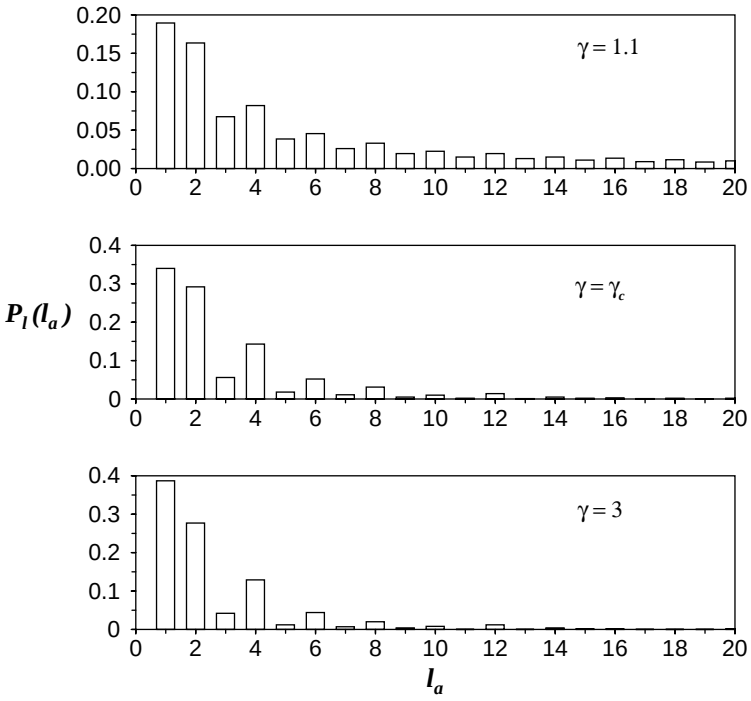

Fig. 12. Probability $P_l(l_a)$ that an arbitrary attractor has a length l_a for networks with $N = 19$. Note that in the chaotic phase the probability $P_l(l_a)$ has a long tail that is absent in the critical and ordered phases.

element to evaluate randomly to 0 or 1 at every time step, independently of the configuration of its controlling elements. The state of the other elements of the network is determined by the dynamical rule given in Eq. (1).

In the absence of noise, the system will fall into an attractor and stay there indefinitely. By introducing noise we can make the system "jump" from one attractor to another. Fig. 14 shows a typical result of the simulation for a scale-free network with $N = 19$. We set $\gamma = 2.5$ and $p = 0.5$ so that the system was in the ordered phase but close to the critical line. For the particular network realization used to construct this figure, the state space broke up into three different attractors that were labeled 1, 2 and 3. Fig. 14 shows the number of the attractor which the system is in as a function of time for two cases: (a) when the random signal is introduced to the element with the highest connectivity ($k = 19$), and (b) when the random signal is forced into an arbitrary element with a low connectivity ($k = 3$). As can be seen from this figure, in the first case the system jumps erratically between the three attractors, whereas in the second case the system spends most of the time in the second attractor. It is interesting to note that in this last case, when the system jumps out of the second attractor, it almost immediately returns to the same second attractor.

Following this method, we can compute numerically the probability $P_j(k)$ of "jumping" between different attractors when an element with connectivity k is perturbed. More precisely, $P_j(k)$ is defined as the number of jumps in a time interval Δt, divided by Δt, when an element with connectivity k is perturbed at every time step. In order to compute this probability, we consider only network realizations for which there are more than just one attractor, and we used $\Delta t = 1000$. Fig. 15 shows $P_j(k)$ as a function of k for scale-free networks with $N = 19$ and different values of γ. The data plotted on this figure are the result of averaging

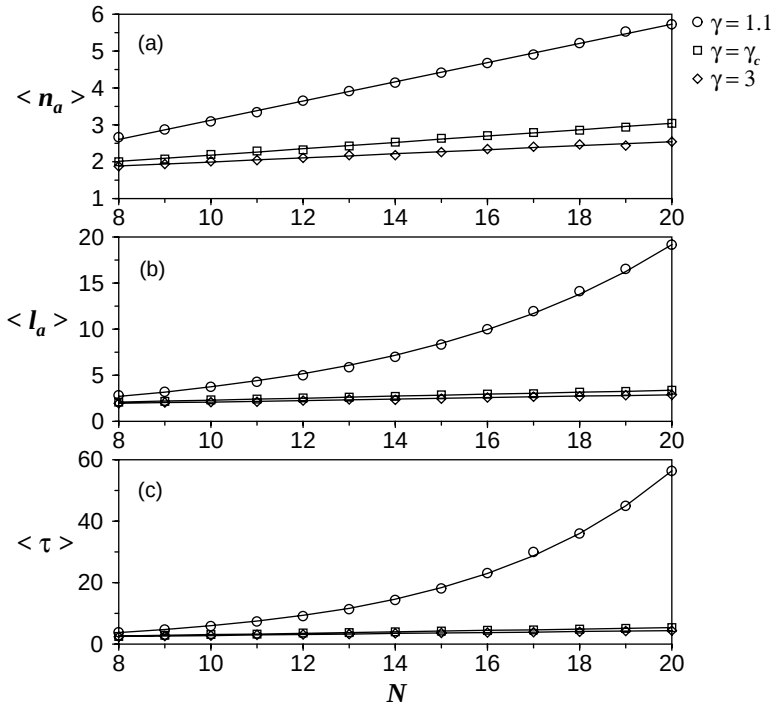

Fig. 13. Mean values of the quantities that characterize the attractor structure of the configuration space, as functions of the size of the network: (a) mean number of attractors $\langle n_a \rangle$; (b) mean attractor length $\langle l_a \rangle$; (c) mean transient time $\langle \tau \rangle$. The three curves in each graph correspond to three different values of γ: chaotic phase ($\gamma = 1.1$—circles); critical phase ($\gamma = \gamma_c$—squares); ordered phase ($\gamma = 3$—diamonds). The symbols are the result of the simulation and the solid lines are the best fit to the corresponding data.

$P_j(k)$ over 20,000 network realizations. It is apparent from Fig. 15 that in the chaotic phase the probability of jumping between different attractors is nearly independent of the connectivity of the element that is been perturbed. This is not the case in the ordered and critical phases, in which $P_j(k)$ increases logarithmically with k.

These results show that in the ordered and critical phases, the stability of the network dynamics in the presence of perturbations depends on the connectivity of the element that is perturbed: the larger the connectivity of the perturbed element, the larger the probability of jumping to a different attractor. This cannot happen in a network with homogeneous random topology since all the network elements are statistically identical. From a biological perspective, the scale-free topology provides the network with both the stability and the evolvability essential for living organisms to adapt and evolve. A scale-free network operating in the ordered phase presents a stable dynamics. Random perturbations (mutations) affecting arbitrary elements of the network do not generally change the network dynamics because the majority of the elements have small connectivities and therefore the probability of jumping to a different attractor is small. However, if these perturbations are produced on a highly connected element, the network performance can change with high probability. These changes can be disastrous for the network functioning, or they can make the system evolve, acquiring a new function.

In this framework, the “life at the edge of chaos” hypothesis is probably not necessary anymore. A scale-free network operating in the ordered phase is generally stable. But it can be forced to a different behavior, probably more advantageous from an

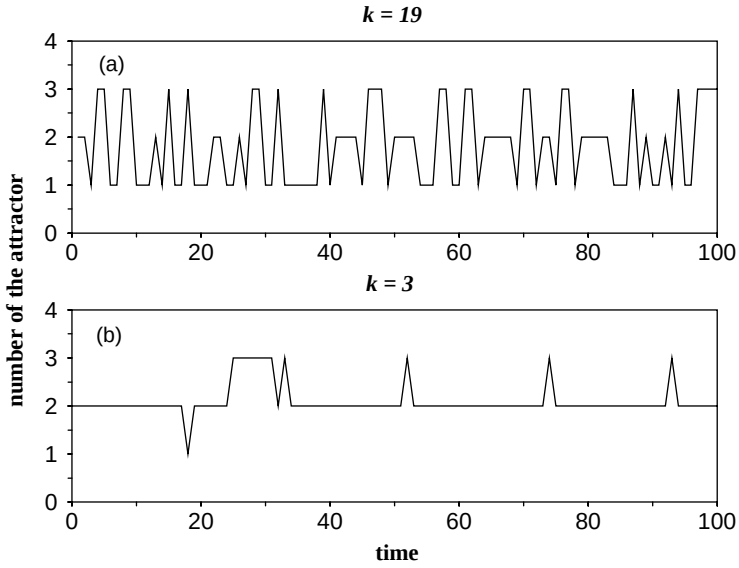

Fig. 14. Stability of the N–K model with scale-free topology when a noisy signal perturbs an element with connectivity k. (a) The system jumps randomly between the three orbits when the random signal is introduced to the element with the highest connectivity. (b) The system is much more stable when an element with low connectivity is the one forced to behave randomly.

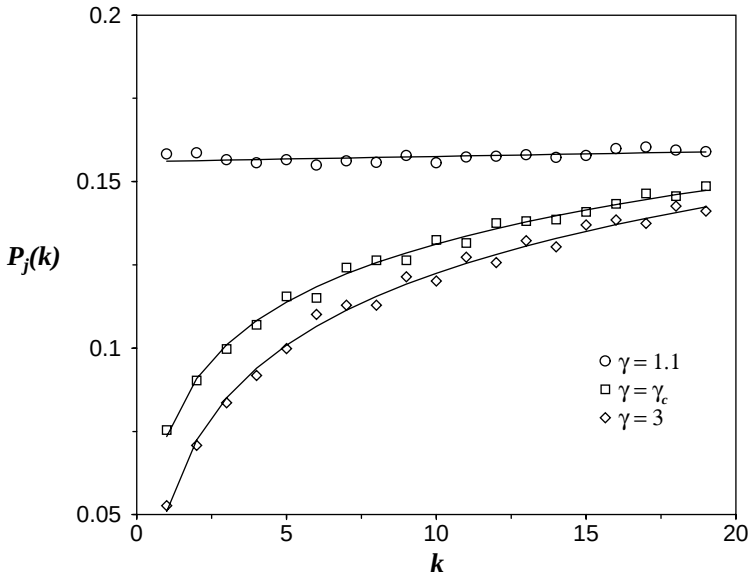

Fig. 15. Probability $P_j(k)$ of jumping between different attractors when a noisy signal is introduced to an element with connectivity k. The data were computed for networks with $N = 19$ taking the average of 20,000 network realizations. The symbols are the result of the numerical simulation and the solid lines are the best fit to the corresponding data.

evolutionary point of view, by perturbing the highly connected elements.

7. Conclusions

A consequence of the scale-free network topology is that the constraint of having a very low connectivity for every element (or a high connectivity with almost constant functions) for the system to be in the ordered phase, is no longer required. The scale-free topology eliminates the necessity of fine-tuning the parameters K and p to achieve stable dynamics. Furthermore, the fact that the phase transition occurs for values of γ in the interval (2, 2.5), allows the existence of elements with a wide range of connectivities in the critical and ordered phases, which is required to describe the observed behavior of real genetic networks. Now that the human genome, as well as the genome of some other organisms, have been thoroughly sequenced, it will be possible to determine experimentally if the topology of real genetic networks is scale-free or not.[7] Although the structures of the configuration space for scale-free networks and homogeneous random networks are qualitatively similar, the scale-free topology is more advantageous from a biological point of view. Scale-free networks operating in the ordered phase exhibit stable dynamics. However, perturbations in the highly connected elements can change the network functioning, allowing the system evolve. Networks with scale-free topology seem to possess the stability and evolvability properties required for living organisms to perform with reliability and to change and adapt to the environment. This result may rule out the hypothesis of life at the edge of chaos. More work is called for to fully characterize the statistical properties of Boolean networks with scale-free topology. We believe that the phase diagram shown in Fig. 4 will be a useful guide for further studies.

[7] Recent preliminary results indicate that the gene-regulatory network of *E. coli*, and the molecular interaction map of the mammalian cell cycle control, have scale-free topologies [12,22]. However, these studies were carried out with partial information of the genetic networks and under the assumption that the important parameter that characterizes the network topology is the mean connectivity rather than the scale-free exponent.

Acknowledgements

I would like to thank Leo P. Kadanoff and Philippe Cluzel for useful and enlightening discussions. I also thank Leo Silbert and Nate Bode for their comments and suggestions. This work was supported by the MRSEC Program of the NSF under award number 9808595, the NSF DMR 0094569, and the Santa Fe Institute of Complex Systems through the David and Lucile Packard Foundation Program in the Study of Robustness.

References

[1] R. Albert, A.-L. Barabási, Statistical mechanics of complex networks, Rev. Modern Phys. 74 (1) (2002) 47–97.
[2] R. Albert, H. Jeong, A.-L. Barabási, Diameter of the world-wide web, Nature 401 (1999) 130–131.
[3] R. Albert, H. Jeong, A.-L. Barabási, Error and attack tolerance of complex networks, Nature 406 (1999) 378–381.
[4] B. Alberts, D. Bray, J. Lewis, M. Raff, K. Roberts, J.D. Watson, Molecular Biology of the Cell, Garland, New York, 1994.
[5] M. Aldana-González, S. Copersmith, L.P. Kadanoff, Boolean dynamics with random couplings, Springer Appl. Math. Sci. Ser., in press. http://arXiv.org/pdf/nlin.AO/0204062.
[6] A.-L. Barabási, Linked: The New Science of Networks, Perseus Publishing, Cambridge, MA, 2002.
[7] S. Bilke, F. Sjunnesson, Stability of the Kauffman model, Phys. Rev. E 65 (2001) 16129.
[8] J. Camacho, R. Guimerá, L.A. Nunes Amaral, Robust patterns in food web structure, Phys. Rev. Lett. 88 (22) (2002) 228102.
[9] B. Derrida, H. Flyvbjerg, The random map model: a disordered model with deterministic dynamics, J. Phys. 48 (1987) 971–978.
[10] B. Derrida, Y. Pomeau, Random networks of automata: a simple annealed approximation, Europhys. Lett. 1 (2) (1986) 45–49.
[11] H. Flyvbjerg, N.J. Kjaer, Exact solution of the Kauffman model with connectivity one, J. Phys. A 21 (7) (1988) 1695–1718.
[12] J.J. Fox, C.C. Hill, From topology to dynamics in biochemical networks, Chaos 11 (4) (2001) 809–815.
[13] S. Huang, D.E. Ingber, Shape-dependent control of cell growth, differentiation, and apoptosis: switching between attractors in cell regulatory networks, Exp. Cell Res. 261 (1) (2000) 91–103.
[14] H. Jeong, B. Tombor, R. Albert, Z.N. Oltvai, A.-L. Barabási, The large-scale organization of metabolic networks, Nature 407 (2000) 651–654.
[15] H. Jeong, S. Mason, A.-L. Barabási, Z.N. Oltvai, Lethality and centrality in protein networks, Nature 411 (2001) 41.

[16] S.A. Kauffman, Metabolic stability and epigenesis in randomly constructed nets, J. Theor. Biol. 22 (1969) 437–467.
[17] S.A. Kauffman, Requirements for evolvability in complex systems: orderly dynamics and frozen components, Physica D 42 (1–3) (1990) 135–152.
[18] S.A. Kauffman, The Origins of Order: Self-organization and Selection in Evolution, Oxford University Press, Oxford, 1993.
[19] B. Luque, R.V. Solé, Phase transitions in random networks: simple analytic determination of critical points, Phys. Rev. E 55 (1) (1997) 257–260.
[20] S. Maslov, K. Sneppen, Specificity and stability in topology of protein networks, Science 296 (2002) 910–913.
[21] M.E.J. Newman, The structure of scientific collaboration networks, Proc. Natl. Acad. Sci. 98 (2) (2001) 404–409.
[22] C. Oosawa, M.A. Savageau, Effects of alternative connectivity on behavior of randomly constructed Boolean networks, Physica D 170 (2002) 143–161.
[23] E. Ravasz, A.L. Somera, D.A. Mongru, Z.N. Oltvai, A.-L. Barabási, Hierarchical organization of modularity in metabolic networks, Science 297 (2002) 1551–1555.
[24] R.V. Solé, J.M. Montoya, Complexity and fragility in ecological networks, Proc. Roy. Soc. Lond., Ser. B 268 (2001) 2039–2045.
[25] R.V. Solé, R. Pastor-Satorras, E. Smith, T.B. Kepler, A model of large-scale proteome evolution, Adv. Complex Syst. 5 (1) (2002) 43–54.
[26] D. Stauffer, Evolution by damage spreading in Kauffman model, J. Stat. Phys. 74 (56) (1994) 1293–1299.
[27] S.H. Strogatz, Exploring complex networks, Nature 410 (2001) 268–276.